Proceedings of the International Conference "Underwater Acoustic Measurements: Technologies & Results"
Heraklion, Crete, Greece, 28th June - 1st July 2005

ANALYSIS OF 3-D ACOUSTICAL EFFECTS IN A REALISTIC OCEANIC ENVIRONMENT

Kaëlig CASTOR[a], Frédéric STURM[b], Pierre Franck PISERCHIA[a]

[a]Laboratoire de Détection et de Géophysique, Département Analyse, Surveillance, Environnement, Commissariat à l'énergie Atomique, BP 12, FR-91680 Bruyères-le-Châtel, France - kaelig.castor@cea.fr / Phone: 33 (0)1 69 26 55 14 / Fax: 33 (0)1 69 26 70 23

[b]Laboratoire de Mécanique des Fluides et d'Acoustique, UMR CNRS 5509, École Centrale de Lyon, 36, avenue Guy de Collongue, FR-69134 Ecully Cedex, France

Abstract: *In this study, numerical simulations of acoustic propagation using a 3-D parabolic equation based model are presented. The calculations are performed on a massively parallel computer with two parallelization levels in order to reduce CPU times for broadband and CW signal propagation. The parallelization procedure is described in detail. Both speedup and efficiency are investigated. CPU times are given for the 3-D ASA wedge benchmark. The parallelized code is then applied to a realistic environment problem involving both sound speed profiles and bathymetry data sets.*

Keywords: *Sound propagation modeling, azimuthal coupling, parallel computation.*

1. INTRODUCTION

In most realistic oceanic problems, the three-dimensional (3-D) environmental variability is weak enough to allow 2-D models to correctly predict sound propagation. However, for some particular environments involving bathymetric slopes or horizontal sound speed gradients, it has been demonstrated experimentally and numerically [1, 2] that 3-D effects can be significant. Fully 3-D models are then needed. Among them, parabolic equation (PE) based models give good results for some benchmark problems. The main drawback is that they can be highly computational time consuming, especially for broadband calculations and/or for long-range paths where the 3-D effects are clearly accentuated. The aim of this work is to solve realistic acoustical propagation problems that were unreachable in reasonable CPU time until now. Numerical simulations are carried out using the 3-D parabolic equation based model 3DWAPE [3, 4, 5] on a massively parallel computer providing a high computational efficiency. The Message-Passing Interface (MPI) communication library is used. In Sec. 2, the 3DWAPE model and its numerical resolution are presented. Section 3 describes the multiprocessing implementation and a validation with CPU-time results

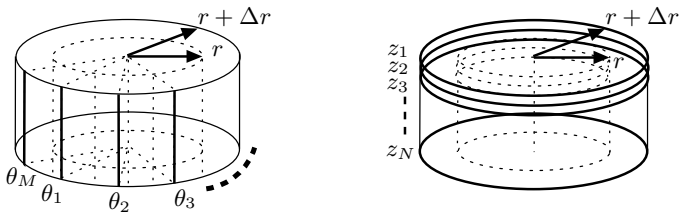

(a) N×2-D part (b) Azimuthal part

Figure 1: *Resolution schemes for (a) Eq. (1) and (b) Eq. (2).*

for the ASA 3-D wedge benchmark. In Sec. 4, an example of realistic oceanic environment in the Mediterranean sea is given. Significant 3-D effects are shown.

2. DERIVATION OF THE 3-D PE BASED CODE 3DWAPE

The 3DWAPE model considers a multilayered waveguide composed of one water layer and one or several fluid sedimental layers. The geometry of each layer is fully three-dimensional. Cylindrical coordinates are used where r, θ, and z, represent respectively the horizontal range, the azimuthal angle, and the depth below the ocean surface. The model calculates the acoustic field $\psi = \psi(r, \theta, z; \omega)$ in the frequency domain satisfying a 3-D parabolic equation splitted as following

$$\frac{\partial \psi}{\partial r}(r,\theta,z;\omega) = \mathrm{i}k_0 \left[\sum_{k=1}^{n_\mathrm{p}} \frac{a_{k,n_\mathrm{p}} \left[(n_\alpha^2 - 1) + \frac{\rho}{k_0^2} \frac{\partial}{\partial z} \left(\frac{1}{\rho} \frac{\partial}{\partial z} \right) \right]}{1 + b_{k,n_\mathrm{p}} \left[(n_\alpha^2 - 1) + \frac{\rho}{k_0^2} \frac{\partial}{\partial z} \left(\frac{1}{\rho} \frac{\partial}{\partial z} \right) \right]} \right] \psi(r,\theta,z;\omega), \quad (1)$$

$$\frac{\partial \psi}{\partial r}(r,\theta,z;\omega) = \frac{\mathrm{i}}{2k_0 r^2} \frac{\partial^2 \psi}{\partial \theta^2}(r,\theta,z;\omega), \quad (2)$$

with $n_\alpha(r, \theta, z)$ the complex index of refraction, $k_0 = \omega / c_\mathrm{ref}$ with c_ref a reference sound speed, and n_p the number of Padé terms. The acoustic field is related to the acoustic pressure by $P(r, \theta, z; \omega) = H_0^{(1)}(k_0 r) \times \psi(r, \theta, z; \omega)$ where $H_0^{(1)}$ denotes the zeroth-order Hankel function of the first kind. Equations (1)-(2) are solved successively at each range step. For a N×2-D computation, only Eq. (1) is considered: A Crank-Nicolson integration in range and an accurate finite-element Galerkin method in depth are used. Let N and M denote respectively the number of mesh points in depth and in azimuth. At each range step, a N×2-D computation requires the inversion of M algebraic linear systems of order N, which corresponds to the acoustic field calculation at successive adjacent azimuths θ_1, θ_2, ..., θ_M, as shown in Fig. 1(a). For a 3-D computation, both Eq. (1) and Eq. (2) must be solved. The azimuthal coupling part handled by Eq. (2) is then discretized using higher-order finite-difference schemes in azimuth, coupled with a Crank-Nicolson type range-stepping procedure. At each range step, the azimuthal coupling part requires the inversion of N algebraic linear systems of order M. As shown in Fig. 1(b), this now corresponds to the acoustic field calculation at successive fixed depths z_1, z_2, ..., z_N. The pulse response at a specific receiver is obtained via a Fourier transform of the frequency-domain solution using

$$P(r,\theta,z;t) = \frac{1}{2\pi} \int_{-\infty}^{+\infty} \widehat{\mathcal{S}}(\omega) H_0^{(1)}(k_0 r) \psi(r,\theta,z;\omega) \mathrm{e}^{-\mathrm{i}\omega t} \, \mathrm{d}\omega, \quad (3)$$

where $\widehat{\mathcal{S}}(\omega)$ is the source spectrum.

3. MULTIPROCESSOR IMPLEMENTATIONS

The total number of arithmetic operations depends roughly linearly on n_p (number of Padé terms) and on the numbers of discrete ranges, depths, and azimuths. Ideally, in a parallel calculation, the CPU times are inversely proportional to the number of processors used. The parallelization strategy chosen in this study consists in separating two principal levels in the distribution of the calculations. Suppose P processors are used. Classically, the *speedup* is defined as the time to complete an algorithm with only one processor divided by the time to complete the same algorithm with P processors. The *efficiency* is defined as the ratio of the speedup over P.

The first parallelization level is specially dedicated to handle efficiently broadband-signal propagation. Computing the time signal at a given receiver requires to perform the following steps: First, the source pulse is decomposed using a Fourier transform. Then the 3-D propagation problem is solved independently at each frequency on different processors. At the end of all the calculations, the frequency-domain solutions at the desired receiver position are collected by only one processor in order to perform an inverse Fourier transform. Note that the communications between processors occur only at the beginning and at the end of the whole process. Communication time is negligible and good performances are thus expected. For instance, if all the P processors are dedicated to the first level, an efficiency close to 100 percent is expected.

The second parallelization level is dedicated to accelerate the calculations at a given frequency. Suppose the acoustic field is known at a given range r. As explained in the previous section, the computation of the solution at the next discrete range $r + \Delta r$ is achieved in two steps corresponding to the N×2-D part and the azimuthal coupling part. The first step requires inverting M algebraic linear systems (Fig. 1(a)). The strategy consists in distributing these inversions on different processors. Once this first step is accomplished, the results of each single processor are re-distributed on the other processors to get prepared for the azimuthal coupling part. The same strategy is then used to invert the N linear systems of the second step (Fig. 1(b)). The results need to be re-distributed between processors before starting the computation at the next discrete range. For this second parallelization level, the efficiency may be limited due to non-negligible communication times.

Both parallelization levels can be combined. Note that several numerical parameter values (*e.g.* Δr, $\Delta\theta$, Δz) depend on the acoustic wavelength. Thus, in order to optimize our parallel calculations, a classical strategy is used to equilibrate the processor workload by using a cyclical repartition of all the frequencies.

The parallelized version of the 3DWAPE code has been validated on several three-dimensional benchmarks [6]. We show here some results for the ASA 3-D wedge shaped waveguide. The source pulse is centered at 25 Hz with a 40 Hz-bandwidth which is decomposed in 281 discrete frequencies. A calculation at 25 Hz requires $M = 3240$ azimuthal points and $N = 500$ depth points. The parallel machine used is a HP SC45 cluster with 214 nodes, each of which contains 4 processors running

at 1.25 GHz and 4 GB of RAM. The maximum computation depth is 1000 m. The reader is referred to Ref. 5 for a detailed description of the relevant benchmark. We present in Table 1 CPU times corresponding to a calculation at 25 Hz and 25 km-range and Table 2 shows the results for the source pulse propagated at 16 km-range. Good performances are obtained. Note that, as expected, the first parallelization level (Tab. 2) provides a better efficiency than the second one (Tab. 1) since fewer communications between processors are required: with 64 processors, a 76 %-efficiency is provided by the first parallelization level whereas the second parallelization level is around 50 to 60 %.

Number of Processors	1	2	4	8	16	32	64
N×2-D CPU time (s)	1245.73	599.61	289.90	143.60	80.67	47.28	34.09
N×2-D speedup	1	2.08	4.30	8.67	15.44	26.35	36.54
N×2-D efficiency	1	1.04	1.07	1.08	0.97	0.82	0.57
3-D CPU time (s)	3121.54	1324.31	596.57	401.60	244.76	142.55	100.13
3-D speedup	1	2.36	5.23	7.77	12.75	21.90	31.17
3-D efficiency	1	1.18	1.31	0.97	0.80	0.68	0.49

Table 1: 3-D ASA wedge benchmark results at a single frequency ($f = 25$ Hz).

Nb. of Proc.	1	2	4	8	16	32	64
4-D CPU t(s)	125992.9	62339.03	34412.10	16926.89	8789.89	4424.57	2583.64
4-D speedup	1	2.02	3.66	7.44	14.33	28.48	48.77
4-D efficiency	1	1.01	0.92	0.93	0.90	0.89	0.76

Table 2: 3-D ASA wedge benchmark results for the pulse propagation.

4. COMPUTATIONS IN A REALISTIC ENVIRONMENT

Realistic numerical simulations are possible using some classical geophysical models for the ocean bathymetry and the sound speed profiles. We illustrate the feasibility of the procedure by focusing on an example in the Mediterranean sea close to the East coast of Corsica (Fig. 2). The Smith and Sandwell data set [7] is used in the following calculations providing an average sampling of 2' (*i.e.* approximately 1.4 km in longitude and 1.8 km in latitude in this region). The GDEM-V data set [8] with a 30' resolution is used to include the 16 sound speed profiles in the region of interest.

A 15 Hz-CW point source is located at 30 m-depth, +42.5°-latitude and +9.7°-longitude. Transmission losses (horizontal slices at 30 m-depth and vertical slices at 90°-azimuth) corresponding to N×2-D and 3-D calculations are shown in Figure 3. At first look, the N×2-D and 3-D solutions seem quite similar by just looking at the horizontal slices. However a closer comparison of these two subplots shows discrepancies mainly in the vicinity of $\theta = 90°$. The vertical slices confirm the significant presence of horizontal refraction effects: The modal structure of the field is strongly modified along the East coast of Corsica. The N×2-D solution clearly shows three propagating modes at all ranges along the $\theta = 90°$-azimuthal direction, whereas the

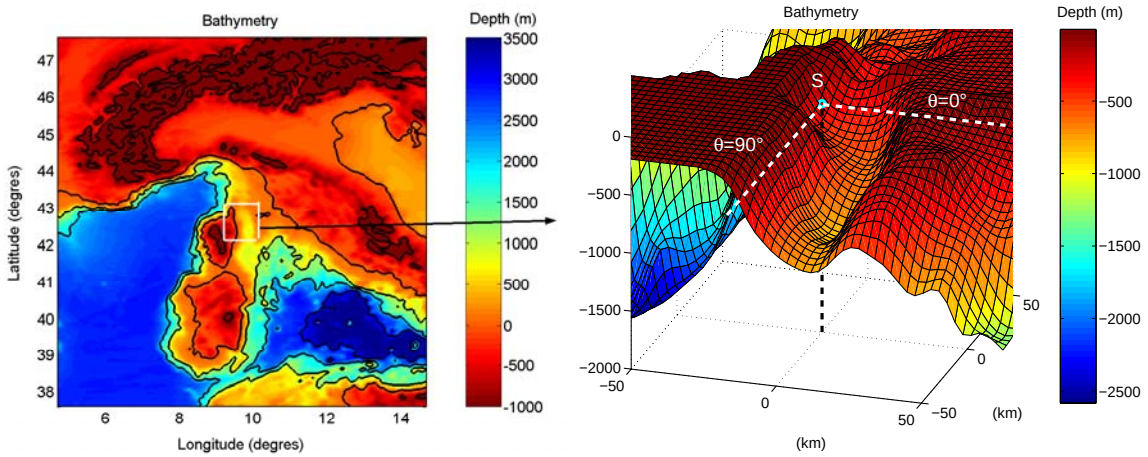

Figure 2: *Maps of the region of interest in the Mediterranean sea (East coast of Corsica).*

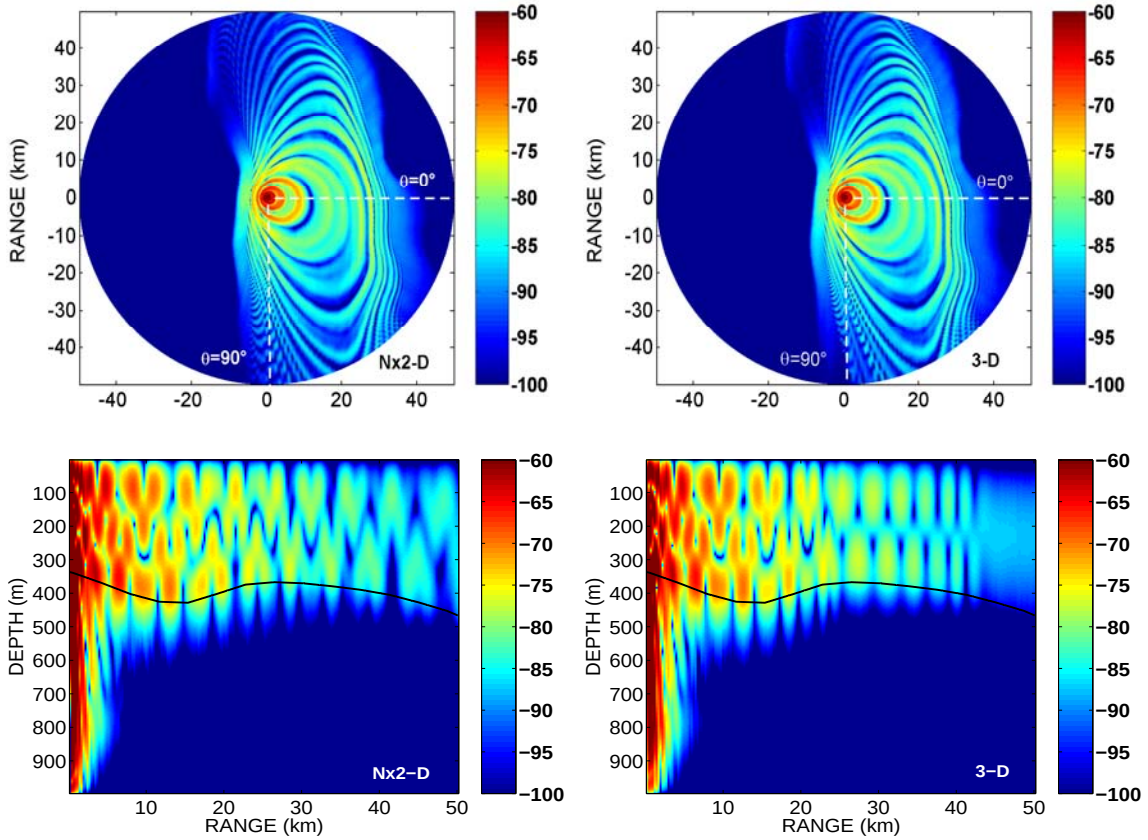

Figure 3: *Transmission loss (horizontal slices for a receiver at* 30 *m-depth and vertical slices for a receiver at a fixed azimuth of* 90°*) corresponding to N×2-D (left plots) and 3-D (right plots) calculations at* 15 *Hz.*

3-D solution exibits an horizontal deviation of the acoustical energy which leads to shadowing effects for mode 3 and mode 2 respectively at 25 km and 45 km-ranges along $\theta = 90°$. These effects are qualitatively the same as the ones that have been analyzed and quantified in detail in ASA 3-D wedge benchmark studies [4] although

the environment parameters considered here are different.

5. DISCUSSION

It is well known that sound propagation modeling in 3-D and/or 4-D is often limited by computational time issues. To overcome this difficulty, an existing 3-D PE code has been implemented in a multiprocessor environment. The parallelization strategy chosen is a suitable two-level procedure. First, a broadband signal calculation is efficiently accelerated by distributing independently on different processors the calculations for each frequency. As expected, good computational performances are obtained in this case since only few communications between processors are needed. The second level of parallelization is dedicated to accelerate the calculations at a single frequency. The distribution on different processors of all the required matrix inversions provides also good results although communications are no more negligible. It is also now possible to use the parallelized version of the code in more realistic configurations including geophysical data: An example has been presented in this paper. We only focused on the acoustic problem at one single frequency. A modal deviation due to a bathymetric slope has been clearly observed in our example. After this preliminary study, future work will be specially addressed to broadband signal propagation in realistic oceanic environments. Reasonable CPU times are expected. Parallel computations overcome CPU time limitations and will make possible analysis of 3-D acoustical effects for different propagation configurations with higher signal frequency and/or propagation distance.

REFERENCES

[1] **S. Glegg, G. Deane, I. House,** Comparison between theory and model scale measurements of the three-dimensional sound propagation in a shear supporting penetrable wedge, *J. Acoust. Soc. Am.*, **94**(4), pp. 2334-2342, 1993.

[2] **C. Chen, J., T. Lin, D. Lee,** Acoustic three-dimensional effects around Taiwan strait: computational results, *J. Comp. Acoust.*, **7**(1), pp. 15-26, 1999.

[3] **F. Sturm**, Numerical study of broadband sound pulse propagation in three-dimensional oceanic waveguides, *J. Acoust. Soc. Am.*, **117**(3), pp. 1058-1079, 2005.

[4] **F. Sturm,** Examination of Signal Dispersion in a 3-D Wedge-Shaped Waveguide using 3DWAPE, *Acta Acustica united with Acustica*, **88**, pp. 714-717, 2002.

[5] **F. Sturm, J.A. Fawcett,** On the use of higher-order azimuthal schemes in 3-D PE modeling, *J. Acoust. Soc. Am.*, **113**, pp. 3134-3145, 2003.

[6] **K. Castor, F. Sturm, P. F. Piserchia,** Acoustical Propagation Modeling Using the Three-Dimensional Parabolic Equation Based Code 3DWAPE within a Multiprocessing Environment, *J. Acoust. Soc. Am.*, **116**(4), pp. 2549-2550, 2004.

[7] **W. H. Smith, D. T. Sandwell,** Global Seafloor Topography from Satellite Altimetry and Ship Depth Soundings, *Science*, **277**, pp. 1956-1962, 1997.

[8] **W. Teague, M. Carron, P. Hogan,** A comparison between the generalized digital environmental model and levitus climatologies, *J. Geophys. Res.*, pp. 7167-7183, 1990.